

RESEARCH ARTICLE

INTEGRATION OF GROUND MAGNETIC METHOD AND WHOLE - ROCK ANALYSIS FOR SOLID MINERAL PROSPECTING IN A PART OF ABUJA, NIGERIA.

Egbelehulu Priscillia* and Abu Mallam

Department of Physics University of Abuja

*Corresponding Author Email: priscilliaegbelehulu@gmail.com

This is an open access article distributed under the Creative Commons Attribution License CC BY 4.0, which permits unrestricted use, distribution, and reproduction in any medium, provided the original work is properly cited.

ARTICLE DETAILS

Article History:

Received 23 July 2024
Revised 09 August 2024
Accepted 24 September 2024
Available online 03 October 2024

ABSTRACT

The ground magnetic survey provides detailed information on subsurface magnetic structures for mineral exploration. This method was carried out within 2.3km by 1.5km of Gwagwalada, Abuja Nigeria bounded by longitude 7°5'20"E to 7°6'40"E and latitude 8°57'50"N to 8°58'40"N in the basement complex of north-central Nigeria. Twenty-five (25) profiles were established over the area at 100m intervals. Data was obtained from the field using a GSM-19 overhauser magnetometer at a time interval of 2s. It was corrected for Diurnal correction and analyzed using Oasis Montaj 8.4 software. The TMI value obtained from the field ranged from 33940.67 nT to a maximum value of 34056.67 nT, and was reduced to the equator. Application of the derivative filters delineated structures that trend NE – SW, E – W, and NW – SE, analysis from the analytic signal filter revealed that the area of study was characterized by varying anomalous magnetic amplitude also it picked up on the magnetic bodies' edges. The location and depth of the structure were determined using the modified dataset and the Euler deconvolution algorithm. The estimated depth of the magnetic source body was about 16.88m to 74.99 m. Rock samples collected during the fieldwork were analyzed; geochemical analysis revealed the possibility of minerals in the area. The result showed that samples are rich in mineral oxides such as iron oxide, titanium oxide, aluminum, and potassium oxides. Samples with the highest silicate value such as quartz as regards the analysis was generally low in other oxides of Fe₂O₃, Al₂O₃, K₂O compared to other samples. This analysis provides vital information on the mineral deposit and structural setting of the study area for possible mineral exploitation.

KEYWORDS

Ground magnetic, derivative filter, mineralization, analytic signal.

1. INTRODUCTION

A geophysical survey is concerned with the inherent and extrinsic characteristics of rocks in every region of the earth, with the aim of retrieving valuable information on the types of natural resources, hydrocarbon fuels, groundwater, and sources of civil engineering and construction problems (Horton, 2003). An essential component of a geophysical survey is paying attention to areas that have anomalous high concentrations of the assets that are being examined. A target of interest can be perceived with the help of the survey's results, or the spatial variation of the property's values can be correlated with variations in the geology of the area (Akingboye, 2018). Consequently, the motive of the geophysical survey is to acquire vital information on the geology, and perhaps locate targets of economic interest, and also bring to light more information about the rock in the area (Egbelehulu et al. 2021).

Geophysical methods thus entail the measurement of rocks properties such as; their susceptibility, conductivity and resistivity, radioactivity, electrical polarizability, density, and seismic velocity (Rajagopalan, 2003; Safronov, 1936). Establishing viable stratigraphic units alongside their host rocks are vital in initiating various exploration projects for a particular mineral or group of minerals. Generally, the major approach for detecting probable mineral deposits on the earth subsurface are basically subdivided into two. A mineral deposit model concerned with the identification of structures, and primary halo method. Mineral deposit model describes the essential geological, geochemical, and geophysical properties and the kinds of minerals they contain descriptively or

genetically, while the second method focus on the spotting of the primary halo of a mineral deposit (Yigui et al., 2022). A considerable large number of mineral deposits are made up of a central zone or core where precious rudiment or minerals are centralized. The zone bordering the core deposit is called primary halo or anomaly that is responsible for the formation of the distribution patterns of the elements as a consequence of primary dispersion. The primary halo is an area that includes rocks, neighboring mineral deposits (ore bodies), and enhance elements that constitute the deposit. A mineral deposit model includes descriptions of primary haloes; however, deposit models and primary halo exploration strategies are entrenched in the study of primary geochemical properties of mineral accumulation. This is because, chemical processes are ultimately responsible for the precipitation of metal or mineral production (Zhao et al., 2011).

Magnetic method plays a vital role in exploring the solid mineral potential in the basement complex. This is because, crystalline basement is made up of rocks which has the highest magnetic susceptibility. Thus, for the purpose of this research, mineral deposit model such as ground magnetic approach to mineral survey is used for identifying likely structures that host minerals since the study area is located within the basement complex of Abuja, while whole rock analysis is used to pinpoint the kind of minerals oxide present in the area. This integration of geophysical and geochemical methods has become necessary in order to reveal mineralized veins and decipher possible mineral within the vicinity of study. The use of magnetic

Quick Response Code



Access this article online

Website:
www.pakjgeology.com

DOI:
10.26480/pjg.01.2024.67.73

methods for mineral exploration is crucial for identifying structures and liable areas of ore deposits, which are important for pinpointing the location of mineralization (Elkhateeb, 2018).

Gwagwalada is one of the suburbs in Abuja, Nigeria known for its vast landmass, dense population and high atmospheric temperature. The hills, valleys and the streams which cuts across them makes it a place of interest for mineral exploration. A lot of the mineral resources in Gwagwalada has not been identified nor completely mapped. Activities of artisanal miners continues to leave a devastating land mass due to their trial-and-error approach in tracing trend and pattern of mineralized vein. It has therefore become important to conduct ground magnetic survey and whole rock analysis to delineate structures present and their mineral potentials. Hence, this research aims at mapping magnetic structures and identifying the mineral potential of a part of Gwagwalada by integrating ground magnetic method and whole rock analysis. The research specific objectives are:

- i. To delineate the magnetic structural setting of the area.
- ii. To estimate the depth of mineralized veins in the research area.
- iii. To identify likeable minerals in the study area from rock analysis.

1.1 Study Area

The research area is located at Gwagwalada in the Federal Capital Territory, Abuja, Nigeria figure 1.0. It is bounded by longitude $7^{\circ}5'20''E$ to $7^{\circ}6'40''E$ and latitude $8^{\circ}57'50''N$ to $8^{\circ}58'40''N$ covering an area of 2.3 km by 1.5 km. The major towns and villages around the area are Giri and Gwako. Settlement in the area is mainly Fulani huts and urbanized residential houses, mostly inhabited by peasant farmers and civil servants. The area is known for artisanal mining activities.

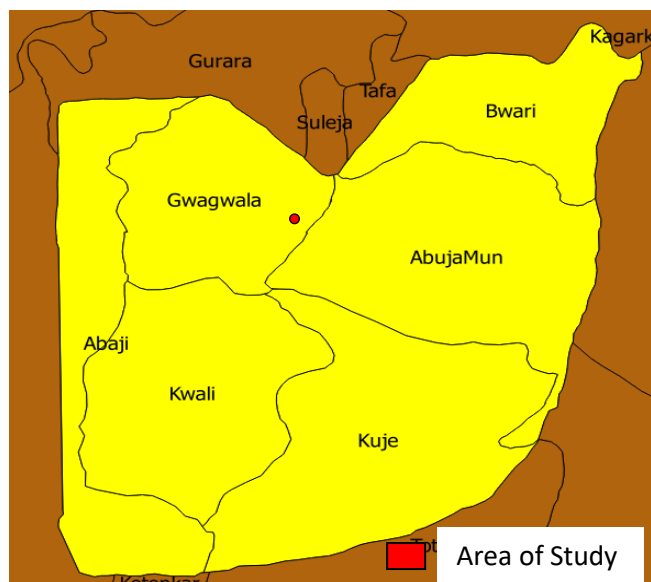


Figure 1: Map of Abuja showing the study area

Source: bit.ly/2utzzns (2019)

2. GEOLOGY OF STUDY AREA

Abuja is described to be supported by mainly two rock formations - the Basement Complex and sedimentary rock formations (Egbelehulu et al., 2021; Bala et al., 2017). The former is made up of undifferentiated Precambrian rocks underlining 90% of FCT distinguished categories of migmatites, Older Granites and meta-sediments. The older-granites are responsible for the rugged relief and rocky landscape found in some parts of the FCT predominantly in the northeast (Offodile, 2003). The basement complex consists of the quartz schists and feldspathic quartz schists. These rocks are identified by their thin covering of stony soils (Mallam and Emenike, 2008). The banded gneisses that dominate the research area shown in Plate 1.0 have well-foliated outcrops that prominently display gneissosity.



Plate 1: Banded Gneiss showing alternation of the mafic and felsic bands

3. METHODOLOGY

Ground magnetic survey covered an area of 2.3km by 1.5 km within Gwagwalada. The area was inspected and profiled, the length of each profile is 1.5 km. The total number of profiles on the area of study is 25 with a space interval of 100 m. A local base station was established where local field gradient was relatively flat, easy to reoccupy, away from suspected magnetic targets or magnetic noise (such as high-tension electric cables, highways, survey car etc.) within the quadrant of study. A GSM - 19 Overhauser advanced magnetometer was used for the survey. The exact time of occupation of each based station was recorded using a GPS.

A representative fresh granite gneiss sample was taken for analyses. Saprolites (weathered host rock) in contact with the quartz materials were also sampled. Rock samples were collected at a depth of about 3m in the crust for analysis. Samples were pulverized and analyzed using X-ray fluorescence spectrometer. Whole rock analysis was carried out on each sample with the use of Induced coupled plasma-mass spectrometer (ICP-MS), which analyses a wide range of element.

3.1 Diurnal correction

A diurnal variation is the term used to describe the continuous shift in the earth's magnetic field caused by its rotation. To remove the effect of this variation in the magnetic data, a base station within the survey area was established, free from likely magnetic interference (Mathu et al. 2015). Magnetic readings were taken repeatedly after every two seconds for the diurnal correction (Rajagopalan, 2003; Mathu et al. 2015). The acquired data was corrected by equations (1) and (2)

$$drift = \frac{B_{bf} - B_{bi}}{t_{bf} - t_{bi}} \quad (1)$$

Where:

Drift is measurement in a loop;

The base station's final and initial total magnetic fields are designated by the letters B_{basef} and B_{basei} .

The base station's final and initial timings are t_{basef} and t_{basei} , respectively.

The drift correction for a day was calculated from:

$$Bdrift_n = B_n - Drift(t_n - t_{bi}) \quad (2)$$

B_n is the total magnetic field at the nth station,

$Bdrift_n$ is the corrected magnetic field,

And t_n is the measuring time there:

The measuring time at the loop's initial station is called t_{base} .

3.2 Magnetic data processing

Magnetic data obtained from the survey area was interpreted by applying various transformation filters and plugs in order to extract structures embedded in the magnetic data set. These application filters and plug are: Reduction to the equator, Derivative filters, and Euler deconvolution plug-in.

3.2.1 Reduction to the Equator

Reduce to the pole operator experiences instability in lower magnetic latitudes due to the singularity displaced by the azimuth of the magnetic source bodies and magnetic inclination which both approaches zero. Thus, at low latitudes, anomaly and noise parallel to the magnetic declination experiences high directionally selective amplification (Ojo et al. 2014; Olaniyan et al. 2012). For this reason, areas closer to the magnetic equator are reduced to the magnetic equator (RTE) instead of to the pole. This operator was applied over the survey data since it's located within areas of low magnetic latitude.

3.2.2 Vertical Derivative

Vertical derivatives highlight shallow or near surface anomalies. This filter highlights high-frequency noise (Mathu et al. 2015) and it was used mainly for delineating structure which formed the basis of magnetic interpretation (Akingboye, 2018).

3.2.3 Horizontal Gradient Derivatives (HGD)

Horizontal derivative (HGD) has the advantage of easy application; noise has little or no interference on it (Pilkington and Keating 2004). It is said to be stable (Scott et al., 2014). However, it has a notable setback of edges dipping, close together (Philips, 2000). HGD is often taken in specific direction which enhances lateral variation of the magnetic field and reduces its regional trend. This derivative gets to its maximum or minimum value in areas which shows prominent and contrasting susceptibility, highlighting discontinuities perpendicular to the direction of deviation, clearing enhancing faults and edges of the structure (Egbelehulu et al., 2021). The magnetic field (M), and horizontal gradient magnitude (HGM) can be deduced by the summation of partial differentiation of M:

$$HGM = \sqrt{\left(\frac{\partial M}{\partial x}\right)^2 + \left(\frac{\partial M}{\partial y}\right)^2} \quad (3)$$

This function stands or gives the peak anomaly above the magnetic contacts if the magnetic field is vertical, magnetization is vertical, contacts are vertical and isolated and the sources are thick.

3.2.5 Euler Depth Estimation

The Euler deconvolution depth estimation plug applied over the data is a useful tool in determining locations and depth for various targets distinguished by a particular structural index. Structural index is the most important parameter in Euler deconvolution. The gradient components of

the magnetic field and their homogeneity are what help locate the source (Joshua, 2017; Mushayandebye et al., 2004). The method applies to some body types, with known structural index. In principle, the method is suitable for various body types. Eigen values obtained in the Euler solution are used to find out if an anomaly is 2D or 3D.

$$x \frac{\partial T}{\partial x} + y \frac{\partial T}{\partial y} + z \frac{\partial T}{\partial z} + NT = x_0 \frac{\partial T}{\partial x} + y_0 \frac{\partial T}{\partial y} + z_0 \frac{\partial T}{\partial z} + NB \quad (4)$$

Where;

x_0, y_0, z_0 are coordinate of magnetic force.

$\frac{\partial T}{\partial x}, \frac{\partial T}{\partial y}, \frac{\partial T}{\partial z}$ are derivatives of total field with respect to x, y, z

N – Structural Index (SI).

B – Regional field

The technique's application is not limited to delineate geologic contacts and faults but it is also used as boundary finder (Ojo et al., 2014; Joshua, 2017). Euler's homogeneity equations provide the foundation for Euler deconvolution.

$$(x - x_0) \frac{\partial M}{\partial x} + (y - y_0) \frac{\partial M}{\partial y} + (z - z_0) \frac{\partial M}{\partial z} = N(B - M) \quad (5)$$

Where:

B is regional value of the total magnetic field

(x_0, y_0, z_0) is the position of the magnetic source which produces the total magnetic field M measured at (x, y, z) .

N is the structural index.

4. RESULT AND DISCUSSION

The TMI map figure 3 of the vicinity of study was produced from the survey data using Geosoft application software. The vicinity of study is marked by magnetic highs and lows. The upper part of the map that is, part of the north central, northwest, and the western part of the TMI map are seen to have short magnetic wavelength with colour aggregate of pink to yellow. The short wavelength signature (high frequency occurrence) observed could be as a result of basement features. While the northeast, eastern part through to the southern part of the TMI map is seen to have average to low magnetic intensity having colour aggregate predominantly green and blue. This long wavelength (low frequency occurrence) is due to a deep magnetic source. The total magnetic intensity value is observed to range from 33931.18 nT to 34065.28 nT within the study area. Structures are seen to be trending NW-SE, E-W and, NE - SW.

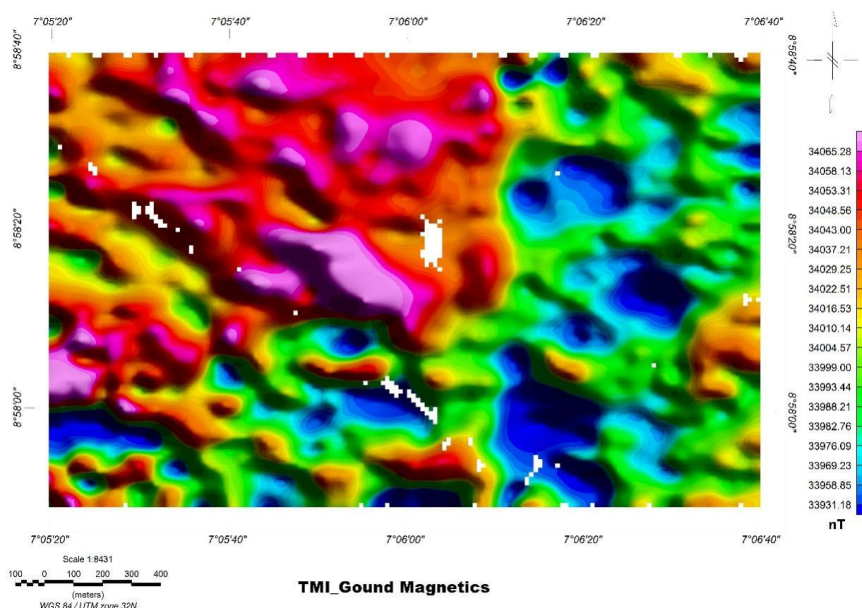


Figure 3: TMI of the Study Area

4.2 Application of RTE on the TMI

The RTE reduction carried out on the TMI (figure 4.11) using Oasis Montaj 8.4 was achieved by the use of these parameters: magnetic total field = 33717.2 nT, magnetic declination = -0.4 and

Magnetic inclination = -7.3. Since the direction of magnetization fluctuates, RTE ensures that the magnetic anomaly is directly located on the causative

bodies (Egbelehulu et al., 2021). On the RTE map (figure 4) it is observed that the sharp demarcation on the TMI (figure 4) at the north central to the northwest from the northeastern part of the map had disappeared, revealing the presence of a near surface structure (short wavelength signature). Edges of structures are refined and sharper. All these features are evident because of the removal of the dependence of the magnetic values on the angle of measurement.

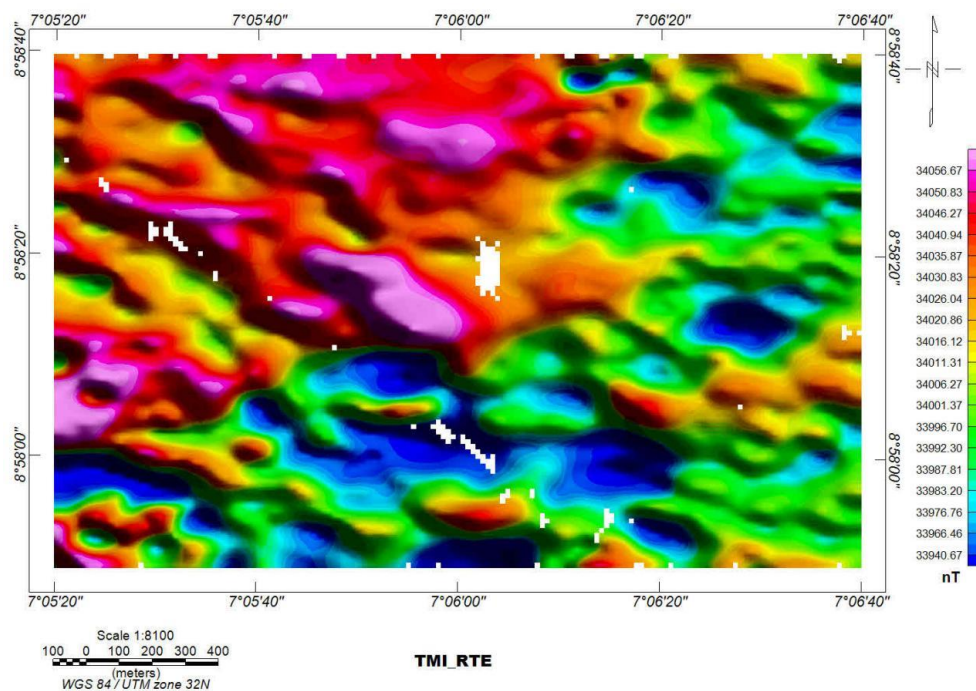


Figure 4: Reduced to Equator Map

4.3 Application of the first Vertical Derivative (FVD)

FVD draws attention to irregularities in bodies and tends to reduce anomalous ambiguity providing a clearer image of the underlying structures causing the anomaly [Nabighian, 1984; Bala et al., 2017]. The filter amplifies short wavelength, thus causative structures can easily be seen but it can sometimes be noisy. The upper part of the RTE map which was predominantly covered by high wavelength signature (red - pink) is replaced with alterations of averagely high (green) to low (blue) wavelength signature, this implies that the signatures are from average to

deep seated structures. FVD map (figure 5) shows clearly areas where magnetic signatures are distorted, and differentiated by various colour contrast on the map. Within these distortions, some notable trends were recognized as zones of linear magnetic high trending E-W, NW- SE and, NE - SW. These magnetic data grid areas with varying resolutions could be interpreted as fractures, dykes, or fault lines. Granite gneiss is the rock type found in the northeastern portion.

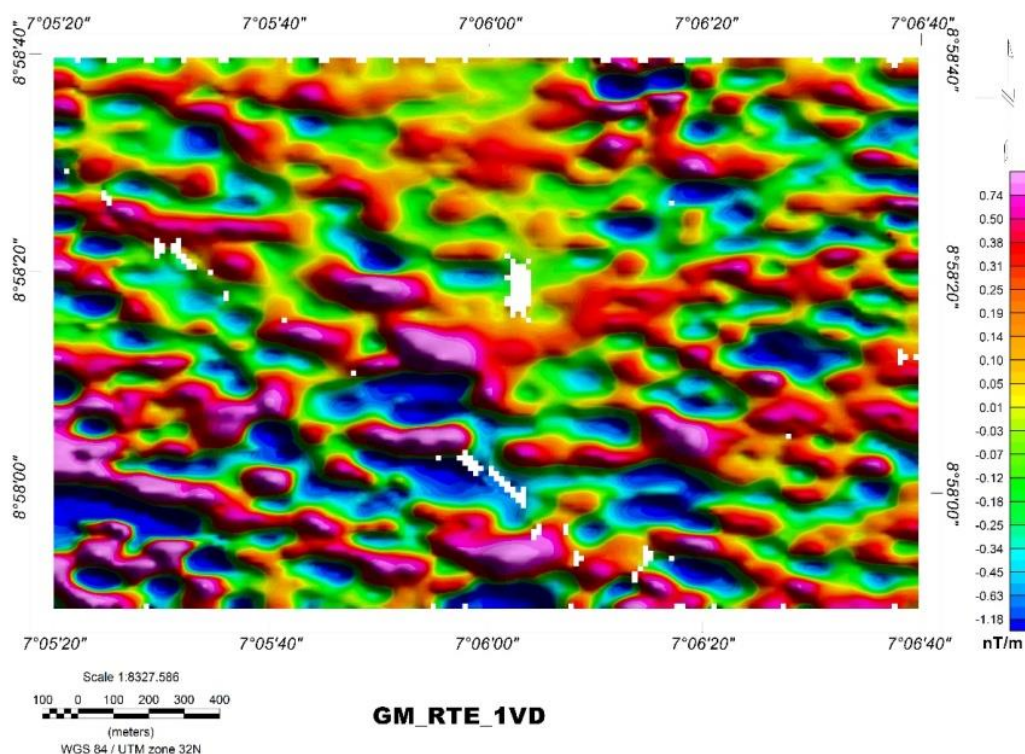


Figure 5: First Vertical Derivative (FVD) map

4.4 Second vertical derivative

The structure shown on the FVD map is highlighted by the second vertical derivative (SVD) in figure 6. The SVD is used to identify dominant structures because it emphasizes local feature expression and cancels out

the effects of big anomalies or regional impacts, ensuring that the magnetic data's zero value closely follows the boundaries of supra-basement disturbances faults. The NE-SW and NW-SE trends are observed to dominate the structure.

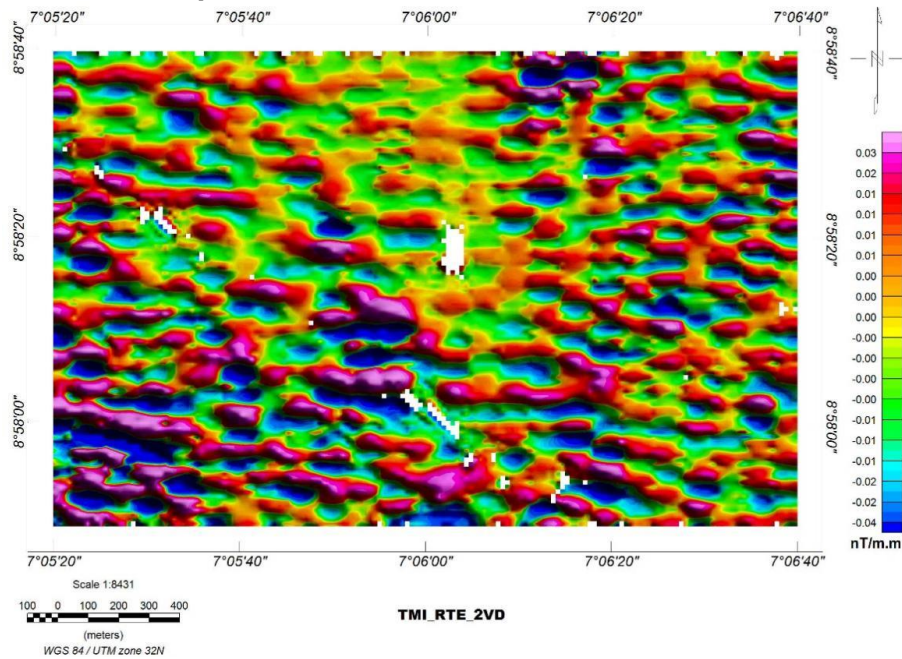


Figure 6: Second Vertical Derivative Map

4.5 Identifying structures from horizontal gradient interpretation

The fault and contact features of the data were strengthened by the Horizontal Gradient (HGRAD) derivative (figure 7). The Horizontal gradient (HGRAD) gave a more specific direction of trend by calculating

the directional gradient. An azimuth is chosen at 90° of the horizontal derivatives counterclockwise to the positive X axis. Compared to the vertical derivative filter, HGRAD has provided a location for faults that is more precise. (Figure 5 and 6). Structures, identified by this filter are clearly trends E – W, NE-SW and, NW-SE.

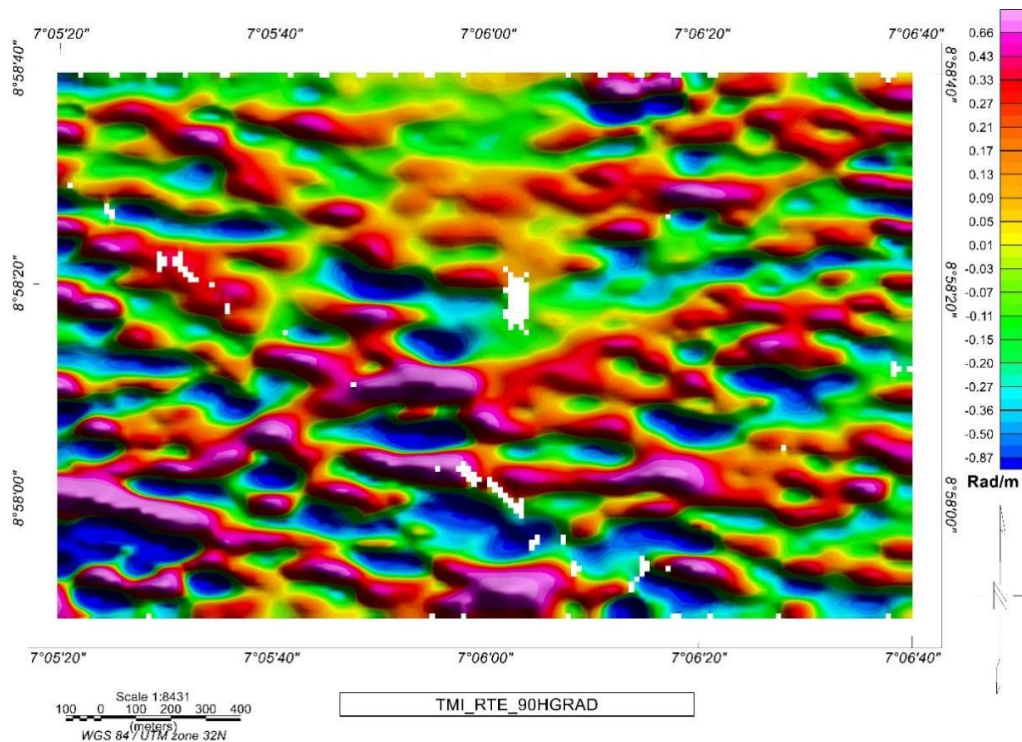


Figure 7: Horizontal Gradient at 90°

4.6 Application of analytic signal

The analytical signal provides a maximum (pink-red coloring) right across distinct bodies and their boundaries, making it more discontinuous than a straightforward horizontal gradient. The output of this filter's application is amplitude domain, as seen in Figure 8. Regions with outcrop has high amplitude values ranging from 1.49 – 0.49 nT/m (pink – red colour) this high amplitude is as a result of outcrop of magnetic rocks. Moderate

amplitudes are represented by yellow to green colouration having values ranging from 0.45 – 0.26 nT/m, the depth could be attributed to intrusion of magnetic basement.

The regions having the least value of amplitude connote areas of magnetic basement intrusion at greater depth. They are identified with sky-blue to deep blue colouration and their values range from 0.22 – 0.09 nT/m.

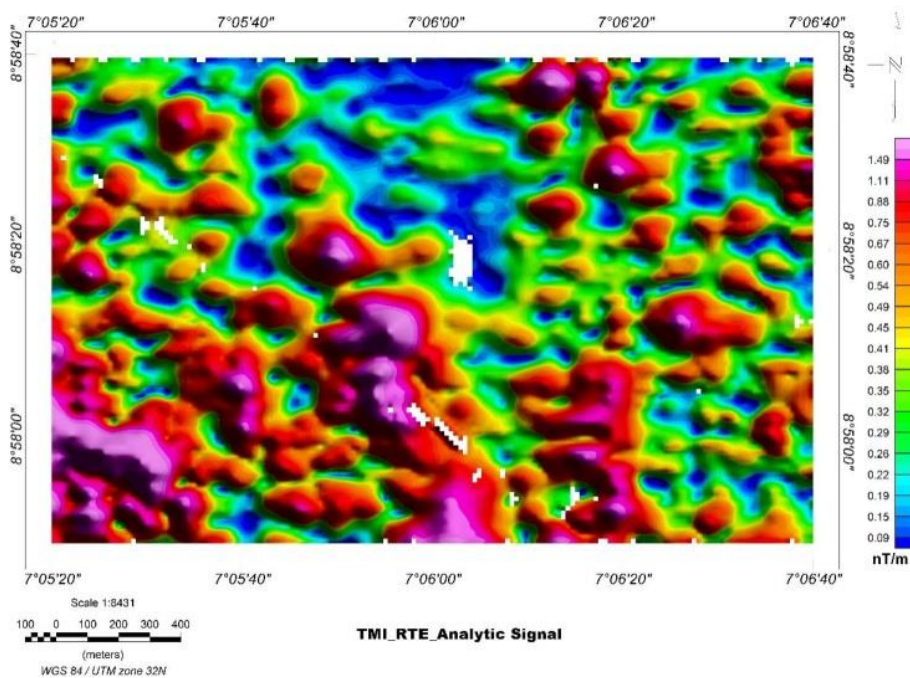


Figure 8: Analytic signal of research area

4.7 Depth Estimation using Euler Deconvolution

The depth of geologic structures was estimated using 3D Euler deconvolution (figure 9). Structural index was chosen to be equal to one (SI=1) since it gave a better clustering of Euler solutions and is more suitable for mapping out depths of structures which happens to be one of the research objectives. The blue cycles represent depth of deep magnetic source which is observed to be distributed within various regions of the research area, and corresponds with structural deduction acquired from the application of derivative filters.

Structures within longitude 7°05'40"E to 7°06'20"E and latitude 8°58'00"N to 8°58'40"N are revealed to have the highest

concentration of blue cycles indicating that there are more structures caused as a result of deep-seated magnetic anomaly compared to other areas. The depth of these structures ranges from 50.81 m – 95.00 m. The yellow –green cycles represent structures of moderate depth whose value ranges from 40.63 m – 48.74 m while the pink – red cycles indicate near surface structures with shallow depth having it values from 28.74 m – 38.79 m.

Structures with these shallow depths are concentrated within longitude 7°05'20"E to 7°05'40"E and latitude 8°57'80"N to 8°58'40"N and agree with the analytical signal map (figure 8) which revealed it as areas having high amplitude.

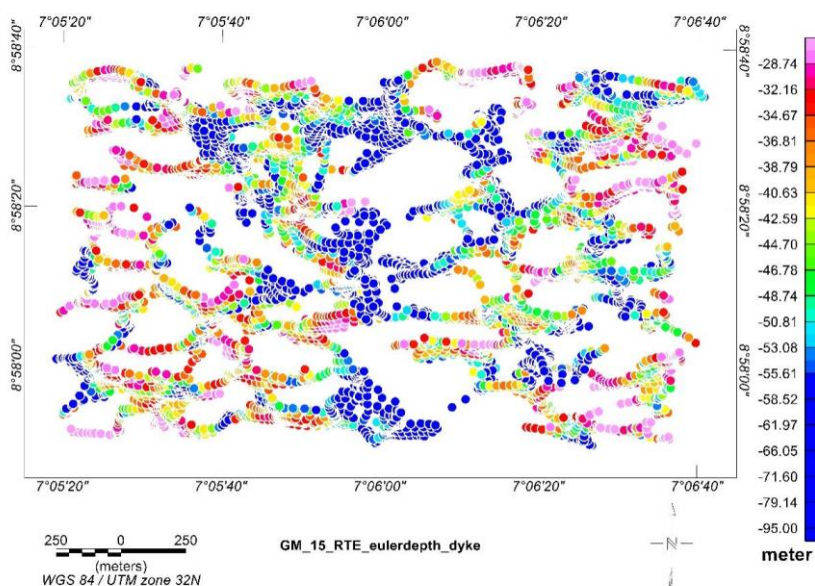


Figure 9: 3D Euler depth of the study area

4.8 Geochemical analysis of rock samples from the study area.

Geochemical analysis carried out on the rock samples was solely to identify contrasts or variations in mineral suites which could be related to sediment provenance since minerals are not completely controlled by source rock mineralogy. Eight (8) rocks samples were collected from the study area as representative rock samples for geochemical analysis which is presented in table1. From the analysis carried out, it is observed that the rocks in the study area are predominantly biotite gneiss and granite gneiss. They cover about 80% of the area and are generally siliceous with

a maximum SiO_2 content of about 99.71 wt. %. Chemical analysis of

minerals are usually expressed as weight percent (wt.%) of its component elements or oxides. The concentration of major element in each sample is measured as %. Sample with the largest SiO_2 content is the quartz having 99.71wt%. This is then followed by Al_2O_3 (Aluminum oxide) which has its maxima value of 18.29 wt. % in granite gneiss and its minimal value in quartz of less than 0.01 wt. %. The next most abundant oxide is Fe_2O_3 (Iron oxide) having a value of 6.72wt. % in granite gneiss and its minimum in quartz having a value of 1.27 wt. %, potassium K_2O is found to have a

value of 5.14 wt.% in Biotite gneiss and less than 0.1 wt.% in quartz. Calcium oxide CaO have a value of 3.34wt. % in granite gneiss and less than 0.01 in quartz. Titanium (TiO_2) has its maximum concentration in granitegneiss with value 1.12 wt. % and its minimum in Quartz of 0.02 wt. %.

From the sample analysis, samples rich in silicate such as the quartz has low concentration of other oxides. The major oxide present in the analysis are silicate, aluminum, iron, potassium and calcium.

Table 1: Whole rock analysis of rock samples

S/N	Name of Oxide	Maximum value in rock sample(wt%)	Minimum Value in rock sample (wt%)
1	Silicate oxide	99.71 (Quartz)	54 (Granite gneiss)
2	Aluminum oxide	18.25 (Granite gneiss)	0.01 (Quartz)
3.	Iron oxide	6.72(Granite gneiss)	1.27 (Quartz)
4.	Potassium oxide	5.14 (Biotite gneiss)	0.1 (Quartz)
5.	Calcium oxide	3.34 (Granite gneiss)	<0.01 (Quartz)
6.	Titanium oxide	1.12 (Granite gneiss)	0.02 (Quartz)
7.	Phosphorous oxide	0.45 (Granite gneiss)	<0.01 (Quartz)

5. CONCLUSION

Total magnetic field intensity data of the area of study was acquired using GSM-19 Overhauser magnetometer covering 2.3 km by 1.5km. Reading was taken every 2 s by the magnetometer along twenty – five profiles. The influence of the solar interaction with the ionosphere was then removed from the acquired data by using the diurnal correction. Low magnetic anomalies are seen to trend linearly in various directions and cut across the entire study area having a minimum value of 33940.67 nT and maximum of 34056.67 nT. Structural analysis was achieved by the application of derivative filters. Structures were revealed to trend NE – SW, E – W and, NW – SE through the application of derivative filters. Analytical signal accentuated the boundaries of outcrops and basement intrusion of moderate depth.

The structures with the greatest depth were determined using Euler deconvolution to be 95.00 m. Deeper magnetic anomalies are as a result of lateral discontinuities in the basement, the intrusion of magnetic basement at much deeper depths, and other features like dykes, fractures, and faults. Shallower magnetic sources were attributed to the presence of outcrops and near surface magnetic structures, which are magnetic rocks identified as granite gneiss. From the interpretation of the magnetic data, it is observed that the study area is highly fractured which makes it liable for mineralization. Analysis conducted on rock samples selected during the ground magnetic data collection reveal that the rocks within the area are rich in mineral oxides such as Aluminum, Iron, Potassium, Calcium and Titanium.

REFERENCE

Akingboye, A. Sunny., 2018. Derivative and analytic signals: Improved techniques for structural classifications. *Malaysian Journal of Geosciences* 2 (1), Pp. 1 – 8.

Bit.ly/2utzns, 2019. Map of Abuja showing the local government area.

Bala, B., Lawal, K. M., Ahmed, A., Umar, M., Mohammed, M. A., and Adamu, A., 2017. The use of Analytic and First Derivative Techniques to gain insight into Aeromagnetic Anomaly patterns in part of Ikara, Nigeria. 2(2), Pp. 684 – 690. (name of journal)

Egbelehulu, P., Mallam, A., Osagie, A.U., and Adewumi Taiwo, 2021. Structural exploration of aeromagnetic data over part of Gwagwalada, Abuja for potential mineral targets using derivative filters. *Journal of*

Geological research. 3(3), Pp. 44 – 51.

Elkhateeb, O.S., 2018. Delineation Potential Gold Mineralization Zone in A Part of Central Eastern Desert, Egypt Using Airborn Magnetic and Radiometric data. *NRIAG Journal of Astronomy and Geophysics.* Pp. 55 – 70.

Horton, R.J, 2003. Application of Magnetic and Electromagnetic Methods to Locate Buried Metal. Open – File Report 3 – 317, U.S Department of the Interior. U.S geological Survey.

Mallam, A. and Emenike, E.A., 2008. Preliminary Findings of Subsurface Characteristics from Direct Current Resistivity Survey of the Federal Capital Territory (FCT) Nigeria. *International Journal of Pure and Applied Sciences.* 2(2), Pp. 68 – 75.

Mathu, E. M., Waswa, A. K., Nyamai, C. M., and Ichang'i, D.W., 2015. Application of magnetic survey in the investigation of iron ore deposits and shear zone delineation: case study of Mutomo-Ikutha area, SE Kenya.

Mushayandebvu, M.F., Lesur, V., Reid, A. B., and Fairhead, J.D., 2004. Grid Euler deconvolution with constraints for 2D structures. *Geophysics*, 69(2), Pp. 489-496.

Nabighian, M. N., 1984. Toward a three-dimensional automatic interpretation of potential field data via generalized Hilbert transforms - Fundamental relations: *Geophysics*, 49, Pp. 780-786.

Joshua, E.O., Layade, G.O., Akinboboye, V.B and Adeyemi S.A., 2017. Magnetic Mineral Exploration Using Ground Magnetic Survey Data of Tajimi Area Lokoja. *Global Journal of Pure and Applied Sciences.* 23, Pp. 301 – 310. www.globaljournalseries.com

Offodile, M. E., 2003. The development and management of groundwater in Nigeria. *Contributions of Geosciences and Mining to National Development*, (NMGS), Pp. 1-7.

Ojo, A.O., Omotosho, T.O. and Adekunle, O.J., 2014. Determination of Location and Depth of Mineral Rocks at Olode Village in Ibadan, Oyo State, Nigeria Using Geophysical Methods. *International Journal of Geophysics.* Pp. 1 – 13.

Olaniyan, O., Abbah, U., Nwonye, N., Aliche, A and Udensi, E.E., 2012. Interpretation of total magnetic intensity field over Bida Basin. *Nigeria Geological Survey Agency. Occupational Paper No (15)*, Pp. 98.

Rajagopalan, S., 2003. Analytical Signal Vs Reduction to Pole: Solution for Low Magnetic Latitudes. *ASEG Extended Abstracts.* 2, Pp. 1 – 4

Safronov, N. I., 1936. Dispersion haloes of ore deposits and their use in exploration. *Problemy Sovetskoy Geologii*, [Problems Soviet Geology] 4, Pp. 41-53.

Scott, W. J., Eng, P., and Geo, P., 2014. *Geophysics for mineral exploration. A manual for prospectors*, 1 (2).

Philips, J.D., 2000. Locating magnetic contacts: A comparison of the horizontal gradient, analytic signal, and local wavenumber methods: *SEG Expanded Abstracts*, 19, Pp. 402-405.

Pilkington, M., and Keating, P., 2004. Contact mapping from gridded magnetic data - a comparison of techniques: *Exploration Geophysics*, 35, Pp. 306-311.

Yigui, L. C., Ndougso-Mbarga, T., Meying, A., and Owono-Amougou, O. U. I., 2022. Detection of sub-surface fractures based on filtering, modeling, and interpreting aeromagnetic data in the Deng Deng-Garga Sarali area, Eastern Cameroon. *Open Geosciences*, 14(1), Pp. 646-662.

Zhao, D., Huang, Z., Umino, N., Hasegawa, A., and Kanamori, H., 2011. Structural heterogeneity in the megathrust zone and mechanism of the 2011 Tohoku- oki earthquake (Mw 9.0). *Geophysical Research Letters*, 38(17).